© Copyright 2000 IEEE. IEEE 51st Annual Vehicular Technology Conference (VTC2000-Spring), May 15-18, 2000, Tokyo, Japan

Personal use of this material is permitted. However, permission to reprint/republish this material for advertising or promotional purposes or for creating new collective works for resale or redistribution to servers or lists, or to reuse any copyrighted component of this work in other works must be obtained from the IEEE.

©IEEE, ISBN: 0-7803-5721-3 51st Vehicular Technology Conference, May 15-18, 2000, Tokyo, Japan

Array Measurement of the Double-directional Mobile Radio Channel

Martin Steinbauer[1], Dirk Hampicke[2], Gerd Sommerkorn[2],
Axel Schneider[2], Andreas F. Molisch[1,3], Reiner Thomä[2], Ernst Bonek[1,3]

[1)] Institut für Nachrichtentechnik und Hochfrequenztechnik, TU-Wien
Gußhausstraße 25/389, A-1040 Wien, Austria
[2)] Technical University of Ilmenau
PO Box 100565, D-98684 Ilmenau, Germany
[3)] Forschungszentrum Telekommunikation Wien (FTW)
Maderstraße 1, A-1040 Wien, Austria
e-mail: martin.steinbauer@nt.tuwien.ac.at

Abstract – We describe a novel technique to measure the *double-directional* mobile radio channel. The channel is called double-directional since it includes directional spreading at both link ends, namely the basestation and the mobile station. We use a *double-array multiplexing technique* consisting of a switched linear array at the receiver and a virtual array at the transmitter site. The measured microcellular scenarios are an open and a closed courtyard with different transmitter positions. The data are evaluated with an *alternating estimation and beamforming* technique that relies on (Unitary) ESPRIT estimation of positional parameters and subsequent beamforming for complex weight extraction. Usage of a two-axis crossed array at the transmitter site avoids forward-backward ambiguity. Presented exemplary results show a good agreement of the extracted directional information with the physical environment and give an indication of its scattering properties.

I. INTRODUCTION

For simulations of adaptive antenna systems, it is essential that the directional behaviour of the channel is modelled correctly [1]. This in turn requires knowledge about the directional spreading at the antenna sites. Channel measurements up to now merely include the directionality at one end of the radio link, either base or mobile station ([2], [3] and references therein). The antenna at the other end is an omni- or a sector antenna. However, for a general characterization the channel must be represented system-independently. For this purpose both the transmitting and receiving antenna used during the measurements must be excluded from the channel.

With *single-directional* measurements, much effort has been made to analyze the angular dispersion at the base station site (e.g. [4], [5]) to estimate the possible gain of smart antenna systems. Some measurements of this kind have also studied DOAs at the mobile station (e.g. [6]), to extract the influence of over-the-rooftop propagation and local scatterers. However, to our knowledge no measurements have been reported where both link-ends *simultaneously* resolve the angular domain. The advantages of such an approach are manifold. It provides (i) the angular dispersion that occurs at the mobile station (MS) for a specific DOA at the base station (BS) and vice versa (*path-dispersion*), (ii) an improved scatterer localization is achieved through triangulization if single scattering is dominant, and, if not (iii) the amount of multiple scattering as compared to single-scattering can be studied. Finally, and most importantly, a double-directional channel description is required for systems with multiple antennas at both the transmitter and receiver sites. Such MIMO (Multiple-Input, Multiple-Output) systems have received enormous interest recently because of their huge capacity [7].

This paper is organized as follows. First, we introduce the *double-directional channel concept* that models doubly angular-resolved channels. The relation between non-directional $\leftrightarrow$ (single-) directional $\leftrightarrow$ double-directional channel responses is derived. In section III, our measurement setup and the double-array multiplexing technique is described, before, in section IV, we turn our attention on the procedure of data evaluation. Having validated the data evaluation algorithm, in section V we present some measurement results.

II. THEORETICAL REASONING

Common directional measurement campaigns presume specific types of antennas, at least at the transmitter. They do not give reliable information on what the channel will be when another antenna is put at the transmitter (TX) site. The logical consequence is to exclude also this antenna from the channel (Fig.

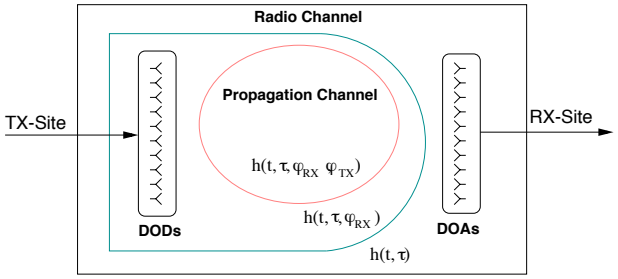

Figure 1: Distinction between radio channel (non-directional) and propagation channel (double-directional). The usual single-directional channel is found in between.

1). While the radio channel is represented by the non-directional channel response (e.g. CIR $h(t,\tau)$), the propagation channel is described by the double-directional channel response. The antenna coherently sums up components from all directions, weighted with the antenna pattern $G(\varphi)$, thus forming the integration over the respective angular domain[1]:

$$h(t,\tau,\varphi_R) = \int_{-\pi}^{\pi} h(t,\tau,\varphi_T,\varphi_R)G(\varphi_T)\,d\varphi_T \quad (1)$$

$$h(t,\tau) = \int_{-\pi}^{\pi} h(t,\tau,\varphi_R)G(\varphi_R)\,d\varphi_R \quad (2)$$

That is, the non-directional CIR $h(t,\tau)$ is the angle integrated directional CIR $h(t,\tau,\varphi_R)$ and the directional CIR $h(t,\tau,\varphi_R)$ is the angle integrated double-directional channel impulse response $h(t,\tau,\varphi_T,\varphi_R)$.

In general the propagation scenario is represented in a system-related fashion by the multidimensional spreading function (MDSF) $s(\nu,\tau,\varphi_R,\varphi_T)$. The latter enters the input-output relationship via a multi-dimensional convolution. Once the characteristics of this function are known for each physically relevant propagation scenario, the behaviour of any system with arbitrary BS and MS antenna configurations can be predicted precisely. Further straightforward enhancements of this principle would include polarization and elevation but are not subject of this paper.

The distinction between different propagation paths between transmitt and receiver (RX) is usually done by their excess-delay τ_i, their Doppler-frequency ν_i and their direction-of-arrival (DOA) φ_R. However, all geometrical paths emanating from the transmitter that have the same Doppler-frequency, delay, and DOA, are summed up. Then, the selection of physical propagation paths is biased by the actual antenna and the effect of this influence cannot be predicted for other antennas.

The double-directional channel model circumvents this problem by separating the following functional blocks in the radio transmission chain[2]:

- the *TX-Antenna*: It distributes the offered signal-energy into the desired directions-of-departure (DOD). These DODs should be selected from the physical input directions offered by the double-directional channel for the specific environment.
- the *Double-Directional Channel*: It includes all resolvable (geometrical) propagation paths between the transmitter- and the receiver-site. Each path is delayed in accordance to it's measured excess-delay τ_i, weighted with the proper complex amplitude $\hat{H}_i e^{j\phi_i}$, and each DOD is converted to the corresponding DOA[3].,

$$h(t,\varphi_R,\varphi_T) = \sum_{i=1}^{N} \hat{H}_i e^{j\phi_i}\delta(\tau-\tau_i)\delta(\varphi_R-\varphi_{R,i})\delta(\varphi_T-\varphi_{T,i}). \quad (3)$$

- the *RX-Antenna*: It collects the signal components from the directions-of-arrival (DOAs) by weighted combination.

To make the most of this channel view, TX and RX antennas need to be smart in some way. Sophisticated DOA-estimation techniques such as MUSIC, ESPRIT or SAGE ([8], [9] ; [10] for a list of references) may be implemented here for weight-vector generation.

III. MEASUREMENT SETUP

We have verified our measurement and modelling approach with an exemplary double-directional measurement campaign in Ilmenau, Germany. A wideband vector channel sounder (RUSK ATM; HIPERLAN/1 band (5.2GHz), bandwidth 120MHz) is connected to a 8(10)-element uniform linear array ($+/-60^o$ element-beamwidth), forming the receiver. The measurement device is described in detail in [11]. At the transmitter side, a virtual array with a monopole antenna excites the channel. The virtual array consists of a X-Y-positioning device with stepping motors. The actual position of the monopole is controlled by the sounder via a serial RS232 interface. The data are captured using a two-sided array multiplexing technique. This cross-multiplexing yields N_T times N_R bursts of complex channel transfer functions. The channel must not change noticeably during the whole measurement period. Each burst consists of 256 consecutive excitations of the channel (Doppler measurement). The regularly sampled data (in frequency, time and two spatial domains)

[1] Only azimuth considered.

[2] From a physical point-of-view, DODs (DOAs) occur at the BS in the downlink (uplink) case and at the MS in the uplink (downlink).

[3] Additive noise omitted.

Figure 2: The channel sounder RUSK ATM and the transmit antenna positioning device.

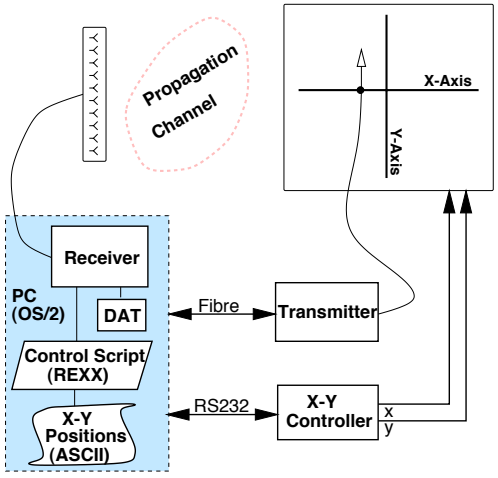

Figure 3: Principle of *Double Array Multiplexing* (DAMUX) for sounding the double-directional radio channel.

are buffered on a harddisk, stored on a DAT-tape, and later transferred to the PC. Figure 2 gives an impression of the sounding apparatus. While a virtual array has the advantage of an arbitrary array-shape, its disadvantage is the very slow measurement-procedure. One complete run (2 x 8 antenna positions at TX times 8 spatial samples at RX times 192 frequency samples and 256 temporal samples gives $16 \times 8 \times 192 \times 256 = 6.291.456$ complex samples) takes about 5 minutes. Estimation of DODs from the spatial samples requires the channel to be static over this amount of time. In order to judge the validity of this prerequisite, we have conducted the same measurement run consecutively 3 times and compared the results. Furthermore, the transmission of bursts rather than single excitations enabled us to perform the necessary exclusion of channel time-variance from the DOD-estimation. Advantage of the virtual array is that – due to the lack of neighbouring elements – no calibration of the array-response as for the physical array is needed.

To properly extract scattering properties, transmitter and receiver must be accurately synchronized in time and frequency. Frequency synchronism and temporal synchronism (necessary to evaluate absolute delays) is maintained through an optical fibre connecting TX and RX. The remaining delay of the triggering event when transferred over the fibre and the processing stages is removed through back-to-back calibration. The measurement setup is shown in figure 3.

IV. DATA EVALUATION

In principle, several methods exist for evaluation of the positional parameters of the multidimensional spreading function (delays, DOAs, DODs). For extraction of delays or Doppler frequencies in most cases the usual Fourier transform with Hanning windowing yields sufficiently accurate estimates. However, DOA estimation from spatially sampled data with Fourier methods is not useful. The low number of spatial samples causes a very low resolution in its dual, the spatial frequency. In addition, the non-linearity of the resulting angular scale causes a large variation of the achieved resolution over the angular range. Due to this reason, high-resolution algorithms are required [10]. For reducing the model order for subsequent estimations from a low number of (spatial) samples, application of superresolution algorithms also e.g. for delay-estimation (s. below) is benefitial. Besides sequential treatment of the different domains, also their joint estimation is possible [12].

Our approach for estimating the spreading function of the channel was the following (Fig. 4): Starting from the 4-dimensional transfer function (time, frequency, space at RX, space at TX), we firstly compute the Doppler-variant transfer function by Fourier transform with Hanning windowing. For elimination of remaining time-variance of the channel, we furtheron use only the 3-dimensional transfer function (the slice at zero Doppler frequency)[4]. This is fed into Unitary ESPRIT [8] to estimate the delays τ_i. (ESPRIT [13] is a parametric subspace-based algorithm for estimating harmonics in additive noise. It therefore inherently needs an estimate of the model order to use for the computation. We used a simple criterion based on the relative power decrease between neighbouring eigenvalues with additional correction by visual inspection of the *Scree Graph* showing the eigenvalues.

Having estimated the parameters τ_i, the corresponding "steering" matrix A_τ can be set up. Subsequent beamforming with its Moore-Penrose pseudoinverse

[4]The scenario was static, the only moving objects were the leaves on surrounding trees. However, we cannot expect to correctly estimate DODs for non-zero Doppler components.

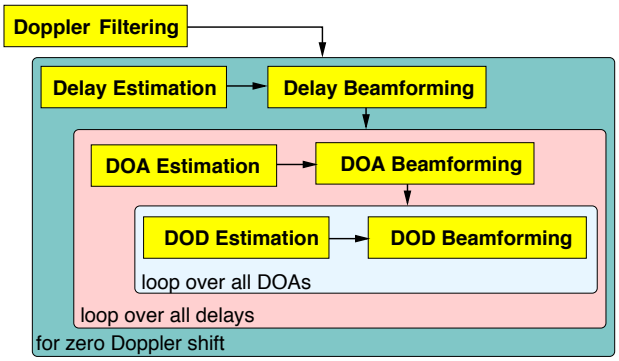

Figure 4: Applied sequential estimation of the parametric channel response in the different domains: *Alternating Estimation and Beamforming*

A_τ^+ gives the parametric 2-dimensional spatial vector channel impulse response $h(\tau_i, x_T, x_R)$:

$$h_{\tau_i}(x_R, x_T) = A_\tau^+ \, T_f(x_R, x_T). \quad (4)$$

After the latter two steps, one dimension, namely the frequency, has been replaced by its parametric dual, the delays. The same procedure (i.e. alternating ESPRIT estimation and beamforming) is now applied consecutively for the DOAs and the DODs so that

$$h_{\varphi_{R,i,j}}(\tau_i, x_T) = A_{\varphi_R}^+ \, h_{x_R}(\tau_i, x_T), \quad (5)$$

$$h_{\varphi_{T,i,j,k}}(\tau_i, \varphi_{R,i,j}) = A_{\varphi_T}^+ \, h_{x_T}(\tau_i, \varphi_{R,i,j}). \quad (6)$$

The information contained in this multidimensional spreading function is the number and values of delays, which DOAs can be observed at these delays and which DODs contribute to each DOA at a specific delay. Through the beamforming step also the complex weights of the underlying MPCs are given by the values of the MDSF at the respective positions. The validity of this approach was checked by means of a synthetical multipath channel with exactly known parameters.

V. MEASUREMENT RESULTS

The following scenarios have been evaluated with the procedure described above:

- *Scenario I: A court-yard with dimensions 26m x 27m, open on one side.* The RX-array broadside points into the center of the yard, the transmitter is located on the positioning device 8m away in LOS.
- *Scenario II: Closed back-yard of size 34m x 40m with inclined rectangular extension.* The RX-array is situated in one rectangular corner with the array broadside pointing under 45^o inclination directly to the middle of the yard. The LOS-connection between TX and RX measures 28m. Many metallic objects are distributed irregularly along the building walls (power transformers, air-condition fans, etc.). This environment looks very much like the back-yard of a factory (s. Fig. 8).
- *Scenario III: Same closed yard as in II but with artificially obstructed LOS-path.* It is expected that the metallic objects generate serious multipath and higher order scattering that can only be observed within the dynamic range of the device if the LOS-path is obstructed.

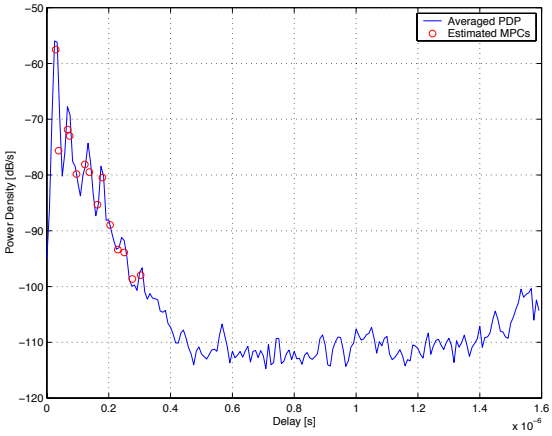

Figure 5: Locally averaged power delay profile for scenario I (LOS).

For the presented evaluations, the virtual TX array had the shape of a cross along x- and y-axis. Both azimuth and elevation were extracted to achieve a higher accuracy in the azimuth estimates[5].

Figure 5 - 7 show the measured power delay profiles (PDP) of scenario I-III. The estimated multipath components, marked by circles, are superimposed. From the plots it is evident that the peaks in the averaged PDP need not correspond exactly to the underlying MPCs [15]. This is partly due to the limited sample size for averaging – there might still exist dominant noise samples – and partly by the remaining bandlimitation of the FFT after windowing the spectrum.

From visual inspection of figures 5-7 we can see that in scenario I there are only a few dominant components while for scenario II,III many more components occur. The PDP in the closed yard is about twice as wide ($\Delta\tau_{\max} \approx 400ns$) as in the one side open yard ($\Delta\tau_{\max} \approx 200ns$) which corresponds well to the maximum geometric dimensions of the yard (max. diagonal scenario I: 38m, max. diagonal scenario II,III: 80m). In the closed yard, a relatively strong late e-

[5] Assuming only incidence in the horizontal plane can cause considerable estimation errors in the azimuth, if there is non-zero elevation [14].

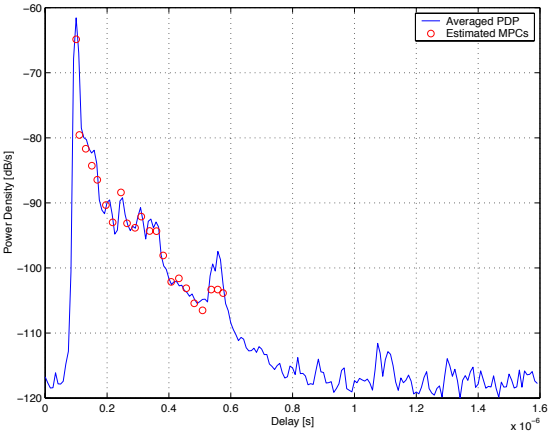

Figure 6: Locally averaged power delay profile for scenario II (LOS).

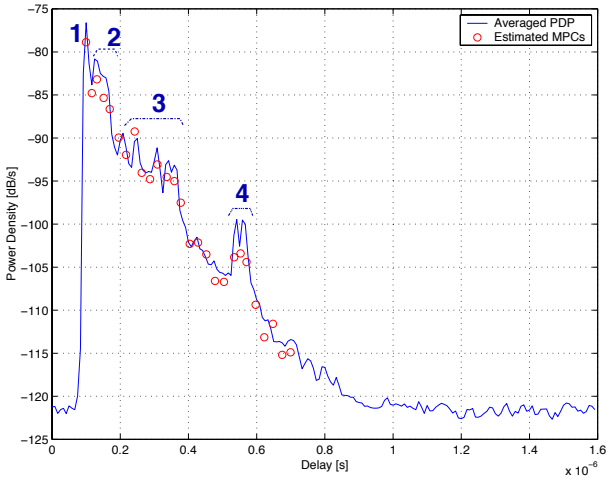

Figure 7: Locally averaged power delay profile for scenario III (NLOS).

cho at 550ns delay is visible. The difference between Scenario II and III is merely an attenuation of the LOS-path by 15dB. The more effective usage of the 40dB dynamic range in the obstructed LOS case does, however, give rise to observance of weak additional MPCs. All PDPs seem to follow an exponential decay.

From the PDP alone, no further interpretations can be drawn; directional information must be taken into account.

To get an idea of the directional spreading properties of the channel, figure 8 shows the extracted directions-of-arrival and -departure (subsequently called DODAs) as rays emanating from the TX and arriving at the RX. This is a top view with correct scaling. The length of the lines representing rays corresponds to the normalized power in dB. From these DODAs in combination with the corresponding delays, 4 different regions have been identified in the PDP (Fig. 7). For each of these regions, one representative path is shown in figure 8. Though obstructed,

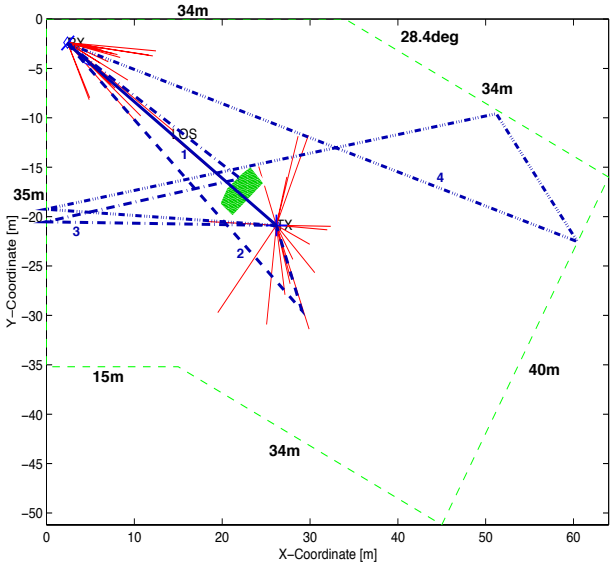

Figure 8: Directions-of-arrival and -departure in top view for scenario III (NLOS).

the direct (QLOS) component (marked by 1) arrives at first and with maximum power. This is reasonable because the obstruction formed by a metallic container was in front of the receiver thereby leaving a low distance for the (cylindrical) diffracted wave to travel. The *second region* (100-200ns) is due to reflections on the back or side of the TX that have LOS to the RX. This is also confirmed by the delay range corresponding to the dimensions of the left-hand ($\approx$ quadratic) part of the yard. *Region 3* (200-400ns) results from second order interactions. This can be concluded only from the additional contemplation of the DODs. From the two directions and the path-length its progression can be extracted accurately. *Region 4* (around 550ns) is made of multiply (specular) reflected components partly due to very grazing incidence on the objects.

While plotting the DODA-specific delay in Fig. 9 serves merely to recognize the LOS component (minimum delay), the 2-dimensional angular power density spectrum shows clearly the amount of power that is carried over a certain DOD-DOA-pair. In Fig. 10 one example for such a 2-dimensional angular power spectral density is depicted for scenario I. For comparison, Fig. 11 shows the angular power spectrum as obtained from a simple Fourier transform. Evidently, the resolution is too poor to give any useful information.

Important for modelling is also the number of multipath components that have to be expected in such an environment. Basically, the number of components depends on the resolution of the system (in delay and angle). However, for practical systems with lower than 120MHz bandwidth (which seems to fit to all actual and near-future systems) the numbers extracted

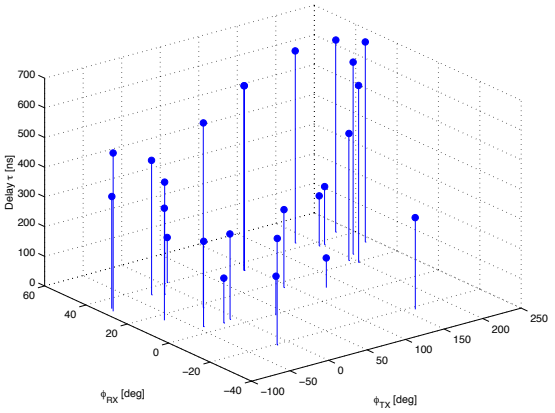

Figure 9: Delay over the directions-of-arrival-and-departure plane (DODA-plane) for scenario III (N-LOS).

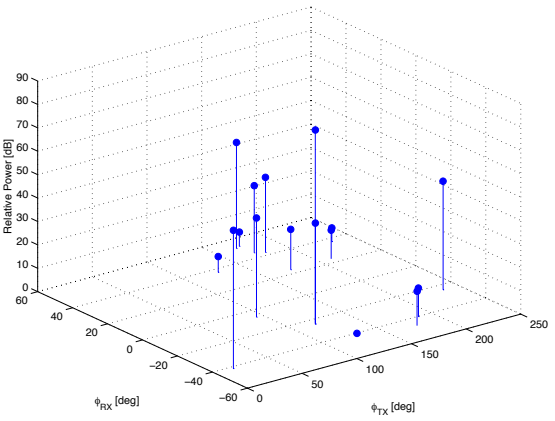

Figure 10: Discrete 2-dim. Power Spectral Density for scenario I (LOS).

from our measurement should be accurate enough. If, for instance, a system uses omni-directional antennas, then the number of delay-only components is characteristic. Our measurement results are summarized in table 1 below. As can be seen, the number of extract-

Parameter	Scenario I	II	III
# Delay Comp.	14	22	27
# Delay-DOA Comp.	20	32	43
# Delay-DOA-DOD Comp.	26	37	54

Table 1: Extracted channel parameters for the measured scenarios.

ed MPCs ranges from 26 to 54, depending on the scenario. This number results from the number of delay components accumulated by the number of DOAs per delay and the number of DODs per DOA. For comparison, the number of delay-only components ranges from 14 to 27. The more components are extracted, the less fading has to be expected for each component.

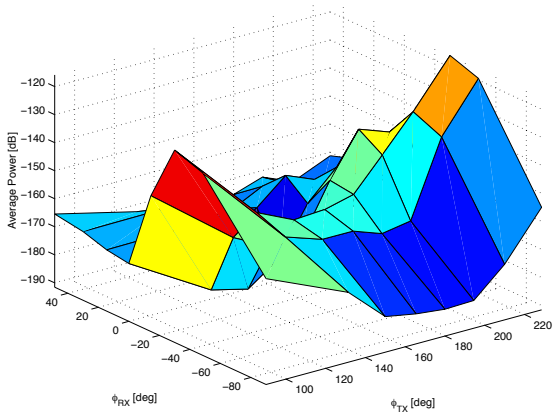

Figure 11: Two-dimensional angular power density spectrum as obtained from Fourier transform (Scenario I).

VI. CONCLUSIONS

We proposed a double-directional channel model that is independent of the influences of the transmit and receive antennas, and allows conclusions about the propagation mechanisms in the channel. Especially, the occurrence and importance of multiple scattering becomes clearly visible. We developed a measurement procedure and data evaluation method that allows to explore such double directional channels, and verified it by an exemplary measurement campaign. The number of multipath components that can be resolved in the delay-DOA-DOD domains is considerably larger (typically by a factor 2) than in the delay domain alone, giving higher possible diversity gain. The angular spread both of the DOAs and DODs is quite large, allowing to anticipate high capacities of MIMO systems in microcellular environments.

ACKNOWLEDGEMENTS

This work has been supported by the European Commission via the project METAMORP under the program "Standards, Measurements and Testing" (Contr.Nr. SMT4-CT96-2093) and the BMBF, Germany, via the project ATMmobil. We thank MEDAV GmbH. for kindly providing us with their channel sounder RUSK ATM for performing the measurements.

REFERENCES

(1) J. Liberti and T. Rappaport, *Smart Antennas for Wireless Communications*. Prentice Hall, 1999.

(2) R. B. Ertel, P. Cardieri, K. W. Sowerby, T. S. Rappaport, and J. H. Reed, "Overview of spatial channel models for antenna array communication systems," *IEEE Pers. Communications Magazine*, pp. 10–22, Feb 1998.

(3) U. Martin, J. Fuhl, I. Gaspard, M. Haardt, A. Kuchar, C. Math, A. Molisch, and R. Thomä, "Model scenarios for intelligent antennas in cellular mobile communication systems - scanning the literature," *Wireless Personal Communications Magazine*, no. 11, pp. 109–129, 1999.

(4) U. Martin, "Spatio-temporal radio channel characteristics in urban macrocells," *IEE Proc. Radar, Sonar and Navigation*, vol. vol. 145, no. 1, pp. 42–49, 1998.

(5) K. Kalliola and P. Vainikainen, "Dynnamic wideband measurement of mobile radio channel with adaptive antennas," *Proc. IEEE VTC'98*, pp. 21–25, 1998.

(6) A. Kuchar, J.-P. Rossi, and E. Bonek, "Directional macro-cell channel characterization from urban measurements," *to appear in IEEE Trans. on Antennas and Propagation*, Feb 2000.

(7) G. Foschini and M. Gans, "On limits of wireless communications in a fading environment when using multiple antennas," *Wireless Personal Communications Magazine*, no. 6, pp. 311–335, 1998.

(8) M. Haardt and J. Nossek, "Unitary esprit: How to obtain increased estimation accuracy with a reduced computational burden," *IEEE Trans. on Signal Processing*, vol. 43, pp. 1232–1242, 1995.

(9) B. Fleury, D. Dahlhaus, R. Heddergott, and M. Tschudin, "Wideband angle of arrival estimation using the SAGE algorithm," *IEEE Conf. Proc. ISSSTA'96*, pp. 79–85, 1996.

(10) H. Krim and M. Viberg, "Two decades of array signal processing research," *IEEE Signal Processing Magazine (Sp.Issue on Array Processing)*, vol. 13, July 1996.

(11) R.Thomä, D. Hampicke, A.Richter, G. Sommerkorn, A. Schneider, and U.Trautwein, "Identification of time-variant directional mobile radio channels.," in *Proc. of 16th IEEE Instrumentation and Measurement Conference IMTC'99*, vol. 1, pp. 176–181, May 1999.

(12) A. Richter, D. Hampicke, G. Sommerkorn, and R. Thomä, "Joint estimation of dod, time-delay, and doa for high-resolution channel sounding," in *Proc. of IEEE Vehicular Techn. Conf., VTC2000 (Spring), Tokyo, May 15-18, 2000.*

(13) R. Roy and T. Kailath, "Esprit – estimation of signal parameters via rotational invariance techniques," *IEEE Trans. on Accoustics, Speech, and Signal Processing*, vol. ASSP-37, pp. 984–995, July 1989.

(14) J. Fuhl, J.-P. Rossi, and E. Bonek, "High-resolution 3-d direction-of-arrival determination for urban mobile radio," *IEEE Trans. on Antennas and Propagation*, vol. 45, pp. 672–682, April 1997.

(15) P. L. C. Cheong, "Multipath component estimation for indoor radio channels," in *Proc. of IEEE Globecom'96*, 1996.